

Synergistic effects of carbon nanotubes and carbon fibers on heat generation and electrical characteristics of cementitious composites

G.M. Kim ^{a,1}, B.J. Yang ^{b,1}, H.N. Yoon ^c, H.K. Lee ^{c,*}

^a Center for Carbon Mineralization, Climate Change Mitigation and Sustainability Division, Korea Institute of Geoscience and Mineral Resources, 124 Gwahak-ro, Yuseong-gu, Daejeon 34132, Republic of Korea

^b Institute of Advanced Composite Materials, Korea Institute of Science and Technology, 92 Chudong-ro, Bongdong-eup, Wanju-gun, Jeollabuk-do 55324, Republic of Korea

^c Department of Civil and Environmental Engineering, Korea Advanced Institute of Science and Technology, 291 Daehak-ro, Yuseong-gu, Daejeon 34141, Republic of Korea

ARTICLE INFO

Article history:

Received 4 December 2017

Received in revised form

13 March 2018

Accepted 22 March 2018

Available online 26 March 2018

Keywords:

Carbon nanotube

Carbon fiber

Cementitious composite

Heat generation

Electrical resistance

ABSTRACT

The heat generation and electrical characteristics of cementitious composites incorporating carbon nanotube (CNT) and carbon fiber under various heating conditions were investigated in this study. Specifically, the synergistic effects of carbon nanotube and carbon fiber on the heat generation and electrical characteristics of cementitious composites were experimentally investigated. The test results show that the addition of carbon fiber improved the heat generation capability and the electrical stability of the cementitious composites incorporating CNT during heating. The long-term durability of construction materials is an important issue, however, there is a practical limit to measuring a property of specimen for a very long time in a laboratory level experiment. In addition, a modified micromechanical model was proposed here to estimate the long-term effect of heating on the electrical characteristics of cementitious composites. The model parameters were derived from the experimental results, and a series of numerical simulations was conducted to explore the influence of model parameters on the resistance of the composites. Comparisons between experimental data and the present predictions were made to assess the potential of the proposed model.

© 2018 Elsevier Ltd. All rights reserved.

1. Introduction

Electrically conductive cementitious composites can be fabricated by adding electrically conductive fillers to cementitious materials [1]. When an input voltage is applied, currents flow through the composites (i.e., conductor) and generate heat. This principle is called Joule-heating mechanism [2]. The electrically conductive cementitious composites have a potential to be applied for the deicing of highways and airport runways, and for floor heating [3].

The conventional fillers often used in the fabrication of electrically conductive cementitious composites include graphite, steel fiber and carbon fiber (CF) [1,4,5]. The conventional fillers have various disadvantages when used as a conductive filler in cementitious composites for heating. For instance, the corrosion of steel

fibers leads to the formation of a passive film on the surface and thereby increases the electrical resistivity of cementitious composites incorporating them [6]. Regarding graphite, a large amount of more than 10% by the weight of cement is needed to ensure the electrical resistivity applicable for heating, though this leads to significant deterioration of the composites [7,8]. In addition, a significant reduction in the electrical resistivity occurs in cementitious composites incorporating conventional fillers at the micro-size level, as the temperature of the composites increased [1,4,5,9]. This phenomenon is known as the negative temperature coefficient (NTC) effect, and an excessive reduction in the electrical resistivity during heating process can cause a thermal shock in the composites [1].

Carbon nanotube (CNT) is a promising nano-material that has outstanding mechanical and electrical properties, and good chemical stability [10–14]. The addition of CNT was shown to contribute to the improvement of the electrical characteristics of cementitious composites in previous studies [15–17]. Kim et al. utilized the cementitious composites incorporating CNT as a

* Corresponding author.

E-mail address: haengki@kaist.ac.kr (H.K. Lee).

¹ These authors contributed equally to this work.

heating material and reported that the heat generation and electrical characteristics of the composites were improved compared to those of the cementitious composites incorporating conventional fillers [18].

However, the homogeneity of the electrically conductive pathways consisting of CNT can be readily damaged by the pore structure in cementitious composites [15,19]. This is attributed that the pores can act as an insulation gap in the cementitious composites [15]. The pore structure is affected by the water to cement (w/c) ratio [20]. Kim et al. reported that the w/c ratio should be minimized to ensure the homogeneity of the electrically conductive pathways in cementitious composites incorporating CNT [16]. Similarly, fine aggregate added to the cementitious composites incorporating CNT may damage the conductive pathways.

Recently, it has been reported in some studies that a combination of CNT and CF as electrically conductive fillers facilitated the creation of hierarchical conductive pathways in cementitious composites and improved its homogeneity [21,22]. Azhari and Banthia reported that the addition of CF to cementitious composites incorporating CNT has a bridging effect between the CF and CNT, resulting in the improvement of the electrical characteristics compared to those of the composites incorporating CNT [21]. However, the effects of Joule-heating on electrically conductive pathways consisting of CNT and CF in cementitious composites have rarely been investigated. Moreover, in-depth studies have not been conducted on the effect of long-term heat generation on the electrical properties of cementitious composites.

The heat generation and electrical characteristics of cementitious composites incorporating CNT and carbon fiber under various heating conditions were investigated in the present study. In addition, a modified micromechanical model based on an effective-medium approach [23,24] was proposed here to predict the long-term electrical properties of the cementitious composites during heating. A series of numerical simulations were conducted to explore the influence of model parameters on the electrical resistance of the cementitious composites. Finally, the present predictions were compared with the experimental measurements to further illustrate the potential of the proposed model.

2. Experimental program

2.1. Specimen preparation

The binding material and the fine aggregate used in this study were type I Portland cement and standard sand described in ASTM C778 [25], respectively. Silica fume (Elkem Inc., EMS-970) and a polycarboxylate type superplasticizer (BASF Pozzolith Ltd., GLENIUM 8008) were used as dispersion agents. The specific gravity and the average diameter of the silica fume were approximately 2.1 and 200 nm, respectively. Multi-walled carbon nanotube (Hyosung Inc. Korea) produced by thermal chemical vapor deposition (CVD) method and PAN-CF (C&Tech., ACECA-3NA1) were used as electrically conductive fillers. The corresponding length and the diameter of the CNT were 10 μm and ranged from 12 to 40 nm, while its purity level and specific gravity were 95% and 1.32, respectively. The diameter and the length of the CF were 7.2 μm and 3 mm, respectively, while its specific gravity was 1.82.

Table 1 shows the mix proportion of the cementitious composites incorporating CNT and CF. Sixteen specimens in total were prepared. The CNT content added to the cementitious composites was varied from 0.3% to 0.6% by weight of the cement, since the percolation threshold values of CNT in cementitious composites ranged from 0.3 wt% to 0.6 wt% in previous studies [17,18]. The CF content ranged from 0.0% to 0.3% by the weight of cement. That is, the replacement ratio of CNT with CF was varied from 0.0% to 50.0%

Table 1
Mix proportion of cementitious composites incorporating CNT and CF (g).

Specimen	Cement	CNT	CF	Fine aggregate	SF	SP	water/cement ratio
N6-50	1000	6	—	500	100	16	0.25
N6-70	1000	6	—	700	100	16	0.26
N6-100	1000	6	—	1000	100	16	0.27
N6-150	1000	6	—	1500	100	16	0.30
N5F1-50	1000	5	1	500	100	16	0.25
N5F1-70	1000	5	1	700	100	16	0.26
N5F1-100	1000	5	1	1000	100	16	0.27
N5F1-150	1000	5	1	1500	100	16	0.30
N4F2-50	1000	4	2	500	100	16	0.25
N4F2-70	1000	4	2	700	100	16	0.26
N4F2-100	1000	4	2	1000	100	16	0.27
N4F2-150	1000	4	2	1500	100	16	0.30
N3F3-50	1000	3	3	500	100	16	0.25
N3F3-70	1000	3	3	700	100	16	0.26
N3F3-100	1000	3	3	1000	100	16	0.27
N3F3-150	1000	3	3	1500	100	16	0.30

according to the weight of the CNT. The content of the fine aggregate was varied from 50.0% to 150.0% by the weight of cement to investigate the effect of the fine aggregate on the homogeneity of the electrically conductive pathways in the cementitious composites during heating. The contents of the superplasticizer and silica fume were fixed at 1.6 wt% and 10.0 wt%, respectively, while the w/c ratio was varied from 0.25 to 0.30 depending on the content of the fine aggregate added.

The cementitious composites with CNT and CF were cast into a cubic mold, as described in ASTM C109 [26]. The size of the cubic mold was 50 mm \times 50 mm \times 50 mm. The fabrication process of the specimens is as follows: the dry materials (selected from cement, fine aggregate, silica fume, CNT or CF) were mixed for 1 min and the solution including the water and the superplasticizer was then added. The mixture was mixed for 5 min and then poured into cubic molds. Two copper electrodes, of which the corresponding lengths and the widths were 70 mm and 30 mm, were inserted into the fresh mixture. The distance between the electrodes was 10 mm and the depth embedded into the specimens was 50 mm. The specimens were demolded and wrapped with polyethylene film after 24 h of curing and then cured at 25 °C for 28 days.

2.2. Test methods

The electrical resistance of the cementitious composites with CNT and CF was measured by a two-probe method using a portable multi-meter (Agilent U1242A). Note that the current applied to each specimen is 0.5 mA when the electrical resistance of the specimen was lower than 1000 Ω [27]. That is, the input voltage of the multi-meter was lower than 0.5 V. A DC power supply was used to apply the input voltage and to measure the electrical current through the cementitious composites with CNT and CF during the heating process. The measured current values were converted into the electrical resistance as $R = V/I$ [18]; where R and V correspondingly denote the electrical resistance and the voltage applied to the specimens and I represents the measured current value through the conductor (i.e., the cementitious composites with CNT and CF). The surface temperature of the composites was measured by attaching a K-type thermocouple on their surface. The thermocouple was linked to a data logger (Agilent Technologies 34972 A) to record the temperature values. The ambient temperature during heating tests was 15 ± 5 °C.

In the present study, three types of heating tests were conducted to investigate the heat generation, the relationship between the electrical and the thermal expansion characteristics of the cementitious composites with CNT and CF, and the heating stability

during a heating process. Input voltages ranging from 5 V to 20 V were applied to investigate the heat generation capability during a monotonic heating test. The input voltages were applied for 30 min, since the temperature increase of the composites was almost saturated within 30 min. A total of ten cycles of tests in a cyclic heating test was conducted for each specimen. For each cycle, the input voltage was applied for 30 min, with natural cooling for a subsequent 30 min. An input power of 12.0 ± 1.0 W was applied to all specimens, since the temperature of the cementitious composites with CNT and CF was proportional to the applied input power [15]. That is, identical amounts of input power for each specimen were applied to investigate the relationship between thermal expansion and electrical characteristics of the specimens at similar temperatures. The applied input power was controlled by varying the input voltage. Two LVDTs were used to measure the thermal strain induced by the Joule-heating during the cyclic heating test. The details of the set up for the cyclic heating test are given in Fig. 1. In a long-term heating test, input power identical to that in the cyclic heating test was continuously applied to the cementitious composites with CNT and CF for 240 h to investigate the heat generation and electrical stability during heating.

3. Experimental results

3.1. Heat generation and tunneling-induced electrical characteristics

Fig. 2 shows the temperature increase in the cementitious composites with CNT and CF as a function of the input voltage. The relationship between the temperature increase in each specimen and the input voltage was linear, meaning that the heat generation capability of the specimen is proportional to the input voltage [15]. The content of the fine aggregate added to the cementitious composites with CNT and CF affected the heat generation capability. The test results show that the temperature increase in the cementitious composites with CNT and CF was reduced as the fine aggregate content increased. This is possibly attributed that the addition of fine aggregate as an insulation gap damaged the electrically conductive pathways in the cementitious composites [28]. Meanwhile, the heat generation capabilities of the N5F1-50 and N4F2-50 specimens were improved compared to those of the N6 series specimens. The heat generation capabilities of the N3F3 series specimens, excluding N3F3-50, were lower than those of the N6 series specimens.

Fig. 3 shows the variation of the tunneling-induced electrical

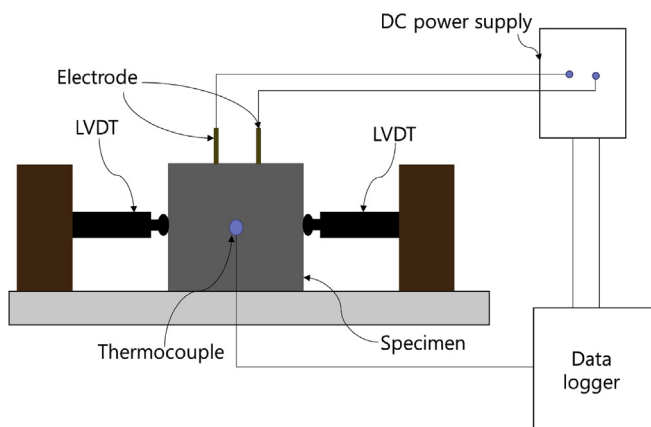


Fig. 1. The schematic of the set up for the cyclic heating test. (A colour version of this figure can be viewed online.)

resistance of the cementitious composites with CNT and CF as a function of the input voltage. The electrical resistance of all specimens was measured within one second when applying input voltage, since the temperature increase in the specimens can affect the electrical resistance [29]. Note that the electrical resistance of the N3F3-150 specimen at 5 V was not recorded, since the current value was lower than the resolution limit of the DC supply used in the test. The test results show that the reduction in the electrical resistance values of the composites became more pronounced as the content of the fine aggregate and the replacement ratio of CF with CNT increased, when the input voltages were applied to the composites. This is possibly attributed that the increase in the content of fine aggregate and the replacement ratio of CF with CNT cause the damage of electrically conductive pathways in cementitious composites [30]. The reduction in the electrical resistance of the composites was possibly caused by the tunneling effect [31]. The tunneling effect is that an activated electrons probabilistically hop an insulation gap, thereby reducing the electrical resistance. The variation of the current density induced by the tunneling effect can be expressed by the tunneling theory equation of Simmons (Eq. (1)), as shown below [31],

$$J = \left[\frac{3(2m\phi)^{\frac{1}{2}}}{2s} \right] (e/h)^2 U \cdot \exp \left[- \left(\frac{4\pi s}{h} \right) (2m\phi)^{1/2} \right] \quad (1)$$

where e and m denote the electron charge and the mass of the electron, respectively, and h represents Planck's constant [31]. U , s , and ϕ are the applied voltage through the barrier, the width of the potential barrier and the tunnel potential barrier height, respectively. It can be inferred from Eq. (1) that the tunneling effect is significantly affected by the distance between the electrically conductive fillers (i.e., the width of the potential barrier). That is, the damaged electrically conductive pathways are favorable for the occurrence of tunneling effect, since the variation of the electrical resistance induced by the tunneling effect occurs when the gap between the electrically conductive fillers is present [30]. The decrease in the electrical resistance of the cementitious composites with CNT and CF led by the tunneling effect was reduced as the replacement ratio of CNT with CF increased. It can be inferred from these results that the CNT content added to the cementitious composites was mainly responsible for the reduction in the electrical resistance induced by the tunneling effect. That is, the possibility of the tunneling effect was reduced when the CNT content added to the cementitious composites decreased, since the addition of CF to the composites with CNT improved the homogeneity of electrically conductive pathways. In contrast, the addition of fine aggregate to the composites deteriorated the homogeneity of the electrically conductive pathways and thus the possibility of the tunneling effect increased [15,30,31].

Fig. 4 shows the relationship between the temperature increase and the electrical resistance of the cementitious composites with CNT and CF at 20 V. The test results indicate that the heat generation capabilities of the cementitious composites incorporating CNT and CF were significantly affected by the electrical resistance when the electrical resistance level is less than 100Ω . That is, a slight increase in the electrical resistance of the cementitious composites with CNT and CF below 100Ω can lead a considerable reduction in the heat generation capability. This is attributed to the fact that the heat generation capability of cementitious composites with CNT and CF is governed by Joule's first law [4]. The relationship between the heat generation capability and the electrical resistance of the cementitious composites with CNT and CF can explain the reason that the temperature increases were clearly different in the composites with a similar tunneling-induced electrical resistance level

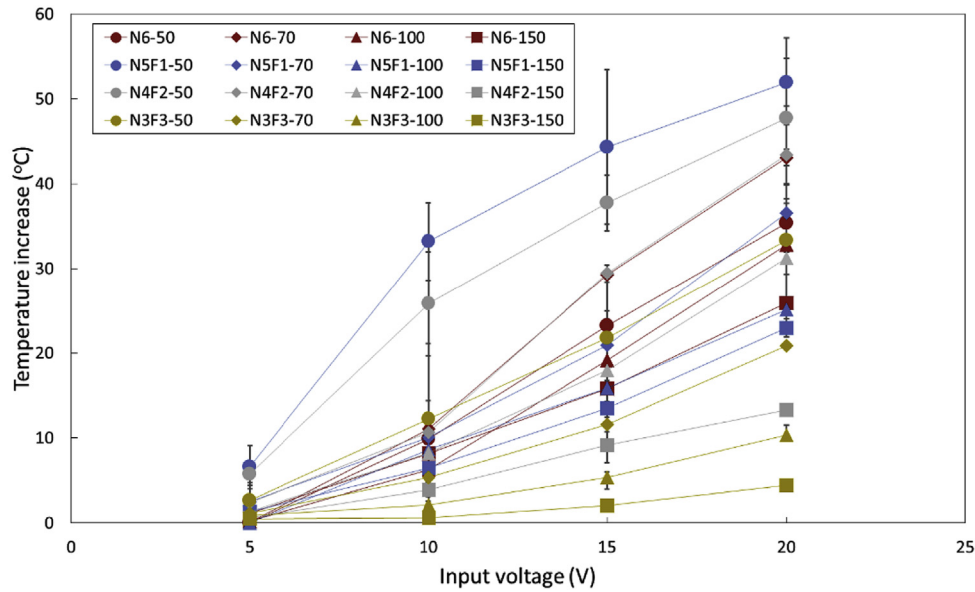


Fig. 2. Temperature increase in cementitious composites with CNT and CF as a function of input voltage. (A colour version of this figure can be viewed online.)

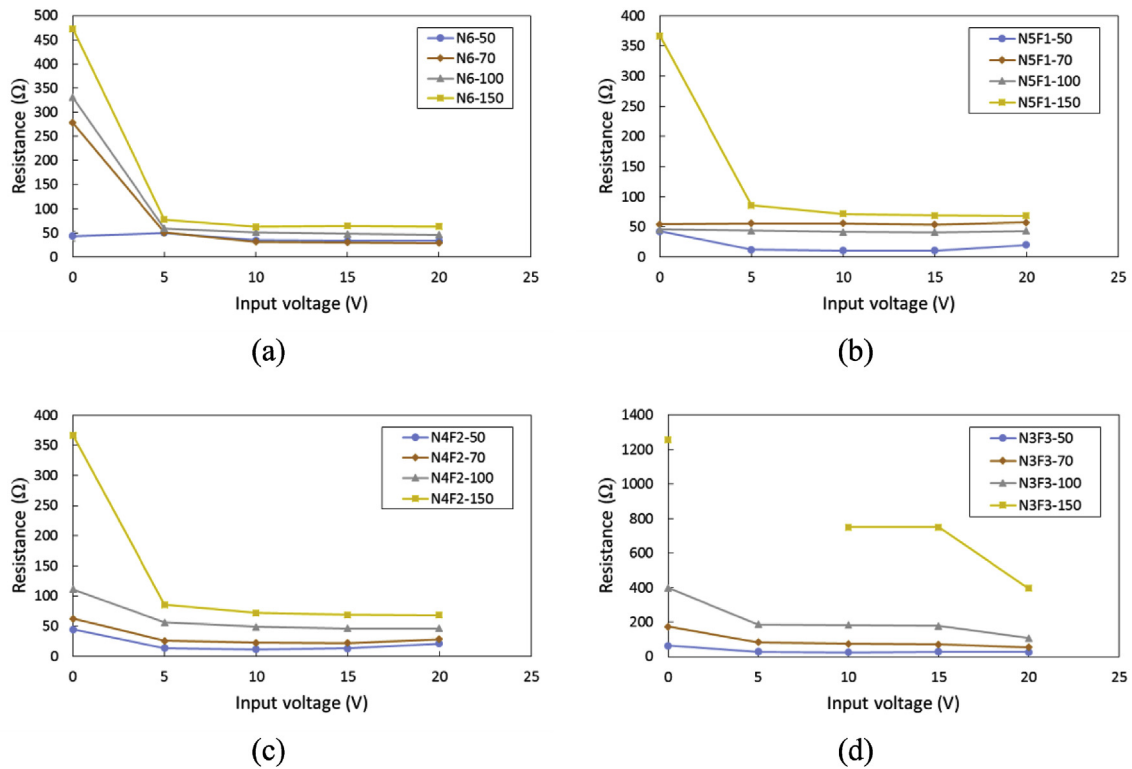


Fig. 3. Variation of tunneling-induced electrical resistance of cementitious composites with CNT and CF as a function of input voltage. (A colour version of this figure can be viewed online.)

(see Fig. (2)). That is, the tunneling-induced electrical resistance of the cementitious composites incorporating CNT and CF below $100\ \Omega$ was slightly increased when the fine aggregate content increased, thereby considerably reducing the heat generation capability.

3.2. Relationship between thermal expansion and heat-induced electrical characteristics

Fig. 5 shows a schematic diagram of the electrical resistance and thermal strain characteristics of the cementitious composites

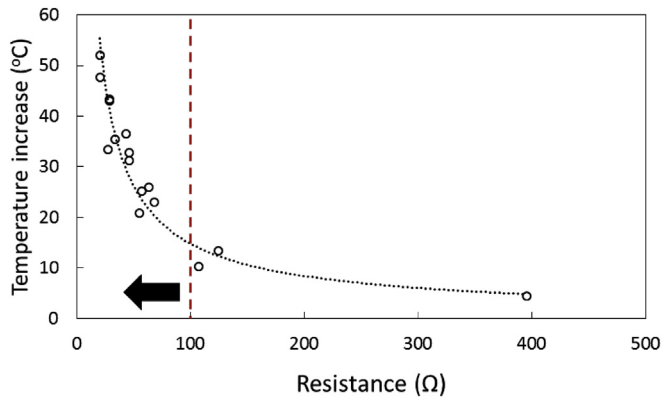


Fig. 4. Relationship between temperature increase and electrical resistance of cementitious composites with CNT and CF at 20 V. (A colour version of this figure can be viewed online.)

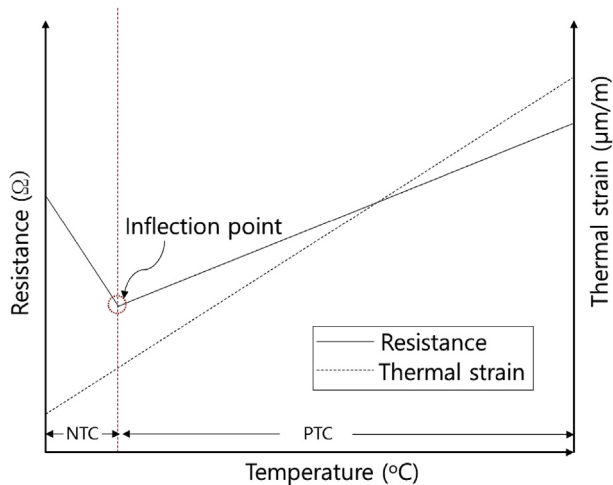


Fig. 5. Schematic expression on electrical resistance and thermal strain characteristics of cementitious composites with CNT and CF as a function of temperature (Kim et al., 2016a). (A colour version of this figure can be viewed online.)

incorporating CNT and CF as a function of the temperature [18]. An increase in the electrical resistance occurs with an increase in the temperature within the area that positive temperature coefficient (PTC) effect arises as shown in Fig. 5 [30,32]. As noted earlier, the NTC effect in previous studies was generally observed in cementitious composites fabricated with conventional electrically conductive fillers such as graphite, CF and steel fiber [5,33]. In contrast, the PTC effect can be observed in cementitious composites with CNT. Kim et al. reported that the NTC effect was observed in cementitious composites incorporating CNT at an initial stage of heating and that the PTC effect subsequently occurred at a relatively high temperature [18]. The occurrence of the PTC effect indicates that the homogeneity of the electrically conductive pathways was damaged by thermal expansion [18]. In the present study, such electrical characteristics associated with an increase in both the temperature and thermal strain were also observed and thus an inflection point was defined as shown in Fig. 5. The occurrence of inflection point indicates that a damage of electrically conductive pathways is initiated, generating the PTC effect [18].

Fig. 6 shows the temperature and the thermal strain of the cementitious composites with CNT and CF at the inflection point during cyclic heating. The occurrence of the inflection point of the

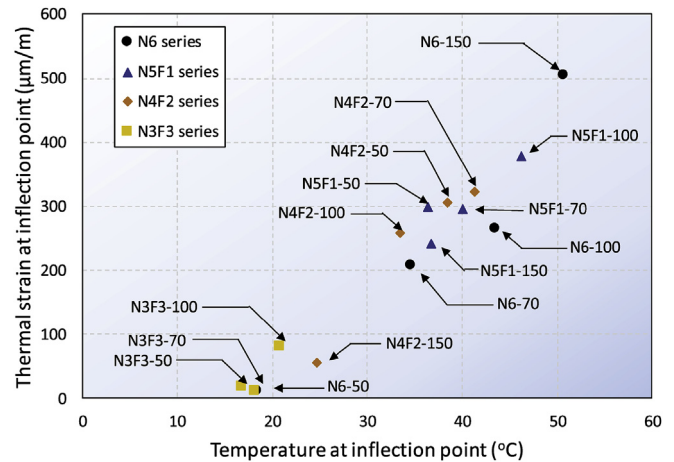
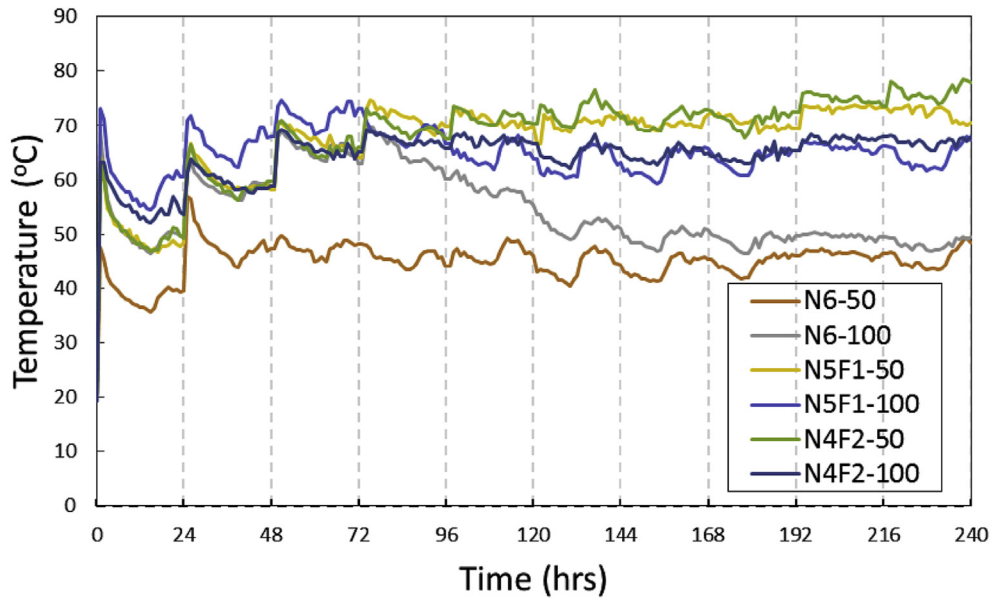


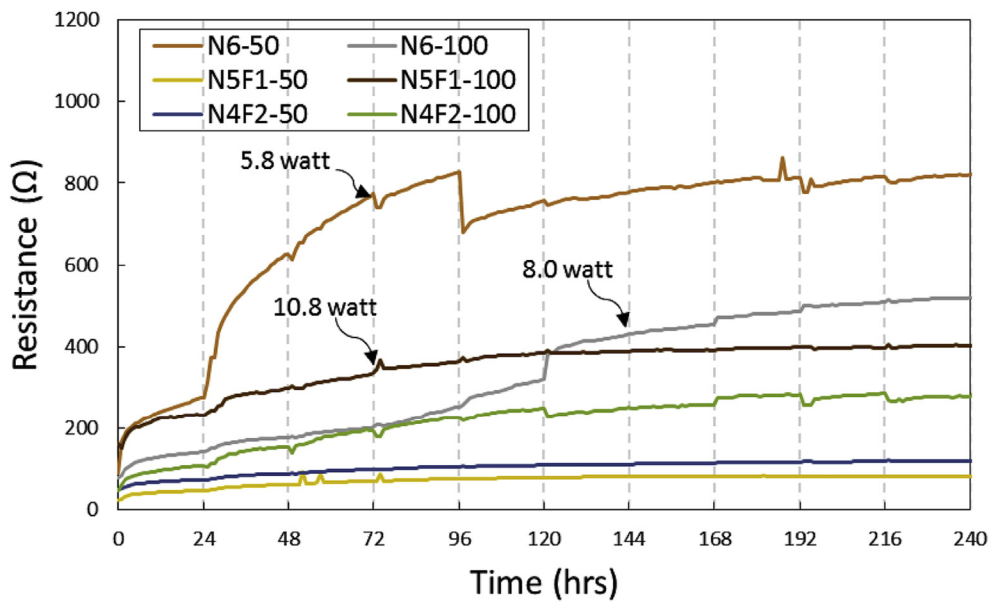
Fig. 6. Temperature and thermal strain of cementitious composites with CNT and CF at inflection point during cyclic heating. (A colour version of this figure can be viewed online.)

N6 series specimens was significantly affected by the fine aggregate content. That is, the temperature and the thermal strain occurring the PTC effect increased as the fine aggregate content increased. This is possibly attributed that the fine aggregate added to the cementitious composites damaged the electrically conductive pathways prior to the heating process [15]. That is, parts of the electrically conductive pathways capable of being damaged by the thermal expansion were reduced by the addition of the fine aggregate. In addition, it is well known that the thermal expansion coefficient of a cement paste is approximately $15\text{--}20 \times 10^{-6}/^{\circ}\text{C}$, while that of a fine aggregate is approximately lower than $10 \times 10^{-6}/^{\circ}\text{C}$ [34,35]. Furthermore, it is well known that the addition of fine aggregate reduces the thermal expansion coefficient of cementitious composites [36]. Consequently, it can be inferred from the fact that the electrically conductive pathways surrounding the fine aggregate were less affected by the thermal expansion [34,35] and thereby increased the temperature occurring the inflection points. However, a further study is needed to investigate relationship between the temperature and thermal strain at inflection point and thermal expansion coefficient.

Meanwhile, the inflection points in the N5F1 series and the N4F2 series specimens, excluding the N4F2-150 specimen, were occurred at a relatively high temperature. In addition, the effect of the fine aggregate content on the occurrence of the inflection point was clearly mitigated. The use of the micro-sized electrically conductive filler in previous studies caused the NTC effect in the electrically conductive cementitious composites during heating process because of the overlapped area between the fillers [1,4,20,37]. That is, the reduction in the overlapped area during heating improved the connectivity among the fillers, showing a reduction in the electrical resistivity of the composites with them. In the present study, the addition of the CF probably formed the overlapped area in the electrically conductive pathways consisting of CNT and CF and the reduction in the overlapped area during heating mitigated the damage of the conductive pathways [37]. Consequently, the occurrence of the inflection point was delayed when the CF was added to the cementitious composites incorporating CNT. In addition, the effect of the fine aggregate content on the occurrence of the inflection point was mitigated since a part of the CF added to the cementitious composites may have passed across the fine aggregate [21].



(a)



(b)

Fig. 7. (a) Temperature and (b) electrical resistance of cementitious composites with CNT and CF during long-term heating. (A colour version of this figure can be viewed online.)

3.3. Heat generation and electrical stability

Fig. 7 shows the temperature and the electrical resistance of the cementitious composites with CNT and CF during the long-term heating. In this test, the applied voltages were changed every 24 h to apply input power of 12 W at the initiation of each day. Note that the input voltage capacity of the DC power supply used in the present study was limited at 60 V. Thus, the input power applied to some specimens was reduced when the initial input voltage to ensure an input power of 12 W was above 60 V. For instance, the applied input power to the N6-50 specimen after 72 h was approximately 5.8 W since the applied input voltage was fixed at 60 V, despite that the electrical resistance of the N6-50 specimen

increased steadily.

The test results show that the temperatures of all specimens were reduced during the initial 24 h. This is attributed that the electrical resistance of all specimens increased within 24 h as shown in Fig. 7(b). In particular, the electrical resistance of the N6-50 specimen significantly increased from 0 to 72 h. Kim et al. reported that an increase in the electrical resistance of electrically conductive cementitious composites was caused by an additional hydration reaction induced by the generated heat and internal cracks resulting from thermal expansion [18]. That is, internal cracks and an additional hydration reaction in the N6-50 specimen likely occurred during the heating step. The temperature of the N6-50 specimen after 72 h was maintained at approximately 45 °C,

since the increase in the electrical resistance was mitigated after 72 h. For the N6-100 specimen, the electrical resistance sharply increased at approximately 120 h. This can be attributed that the occurrence of internal cracks damaged the electrically conductive pathways consisting of CNT. The temperature of the N6-100 specimen was steadily reduced up to 144 h owing to the steady increase in the electrical resistance. In contrast, the electrical resistance of the N5F1 series and N4F2 series specimens within 24 h slightly increased and then became stable, thereby mitigating the temperature reduction in these specimens. Meanwhile, the temperatures of the N5F1-50 and the N4F2-50 specimen were higher than those of the N5F1-100 and the N4F2-100 specimens. The improvement of the heat generation capability in the N5F1-50 and the N4F2-50 specimens was attributed that the increase in the electrical resistance during heating was less than those in the N5F1-100 and the N4F2-100 specimens. That is, the addition of CF to cementitious composites with CNT improved the homogeneity of the electrically conductive pathways and probably created an overlapped area in the pathways. The overlapped area in the electrically conductive pathways consisting of CNT and CF enabled to resist the damages induced by thermal expansion during heating and an additional hydration reaction. Consequently, the characteristics of the electrically conductive pathways consisting of CNT and CF improved the heat generation and electrical stability of the composites.

Overall, the electrical and heat generation characteristics of cementitious composites during heating process was closely related to the matrix change induced by the thermal expansion. The combination of CNT and CF mitigated the damage resulting from the thermal expansion and improved electrical and heat generation characteristics of cementitious composites, since the combination created homogenous electrically conductive pathways with an overlapped area in the composites. Meanwhile, the fine aggregate acted as an insulation gap, reducing the homogeneity of the electrically conductive pathways in cementitious composites. However, the combination of CNT and CF reduced an adverse effect of fine aggregate on the electrical and heat generation characteristics of the composites.

4. Prediction of long-term electrical properties of cementitious composites

The long-term electrical conductivity (σ) of cementitious composites is estimated through the effective-medium theory [23,24,38]. The adopted theory is modified in the present study to reflect the characteristics of the present cementitious composites, and thus the following four assumptions were considered (Fig. 8):

(1) the CNT and CF are thinly coated with electrical resistivity, (2) the aspect ratio of CNT is varied according to the degree of CNT waviness, (3) the curved CNT gradually expands as the temperature in the cement composites increases, and (4) the tunneling region can be transformed to various sizes by heat-generation. The derivation process and the implicit equation of the effective-medium theory are given in Eqs. (1)–(3) and Eq. (8) of [23]. The above-mentioned assumptions can be applied by replacing the length of CNT ($L(\theta)$) and scale parameter (γ) of the effective-medium theory with the following equations:

$$\begin{cases} \theta = \frac{6K \cdot t + 3K + 20}{10(2t + 1)}, \quad \gamma = K \cdot T \cdot t, & \text{if } \phi_{CF} = 0 \\ \theta = \frac{2(30t + K + 15)}{K(2t + 1)}, \quad \gamma = K \cdot T \cdot \left(\frac{1}{\exp(\phi_{CF} \cdot t^2)} \right), & \text{if } \phi_{CF} \neq 0 \end{cases} \quad (2)$$

where K , T , and t are the thermal expansion coefficient, temperature, and time, respectively; θ is the waviness factor that affects the length of CNT and is defined in Eq. (8) of [15]; ϕ_{CF} signifies the volume fraction of CF.

To represent the influence of model parameters on the resistance of composites, a series of numerical simulations is carried out and presented in Fig. 9. The material and model parameters are: $\sigma_{\text{Cement}} = 5 \times 10^{-5} \text{ S/m}$, $\sigma_{\text{CNT}} = 1.943 \times 10^4 \text{ S/m}$ [39], $\sigma_{\text{CF}} = 1.0 \times 10^3 \text{ S/m}$; $L_{\text{CNT}} = 10 \mu\text{m}$, $d_{\text{CNT}} = 26 \text{ nm}$, $L_{\text{CF}} = 3 \text{ mm}$, $d_{\text{CF}} = 7.2 \mu\text{m}$; $\phi_{\text{CNT}} = 0.5\%$, $\phi_{\text{CF}} = 0.1\%$, $\theta = 3^\circ$, $K = 15 \times 10^{-6}/^\circ\text{C}$, and $T = 0.005t + 60^\circ\text{C}$. First, the electrical resistance-time relation of the composites incorporating CNT or CNT/CF is shown in Fig. 9(a). It shows the typical electrical properties that the resistance of CNT/composites gradually increases over time, while the constant increase in resistance is mitigated when the CNT and CF are simultaneously incorporated into the composites [40]. It is due to the synergistic effect from CF, bridging the conductive networks of CNTs. The detailed descriptions of the synergistic effect are covered in the experimental section, and the proposed model closely simulates such phenomena, as shown in Fig. 9(a). Fig. 9(b) and (c) show the resistance of composites as a function of the time. It is seen that the cementitious composites with high volume fraction of CNT and CF fillers become more conductive materials [41]. It is also observed that the bridging phenomenon appears earlier and the electrical improvement is more pronounced as the volume fraction of CF increases.

The present prediction is compared with the experimental measurements to assess the potential of the modified model. The comparison with the prediction is based on the experimental data shown in Fig. 7, and the results are given in Fig. 10. The applied values of ϕ_{CNT} , ϕ_{CF} , and K in the predictions are summarized in

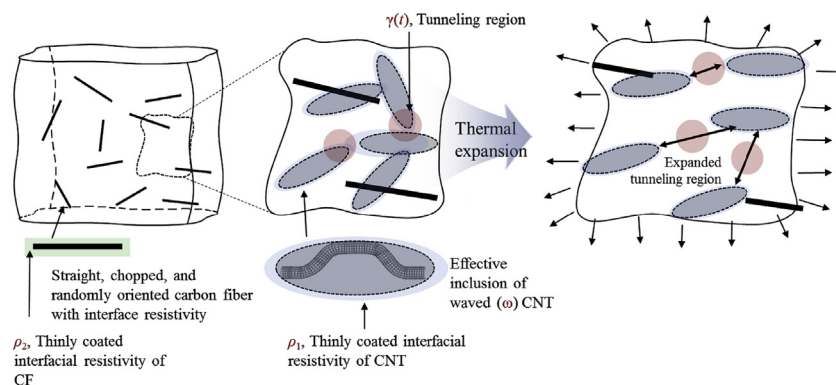


Fig. 8. Schematics of the cementitious composites. (A colour version of this figure can be viewed online.)

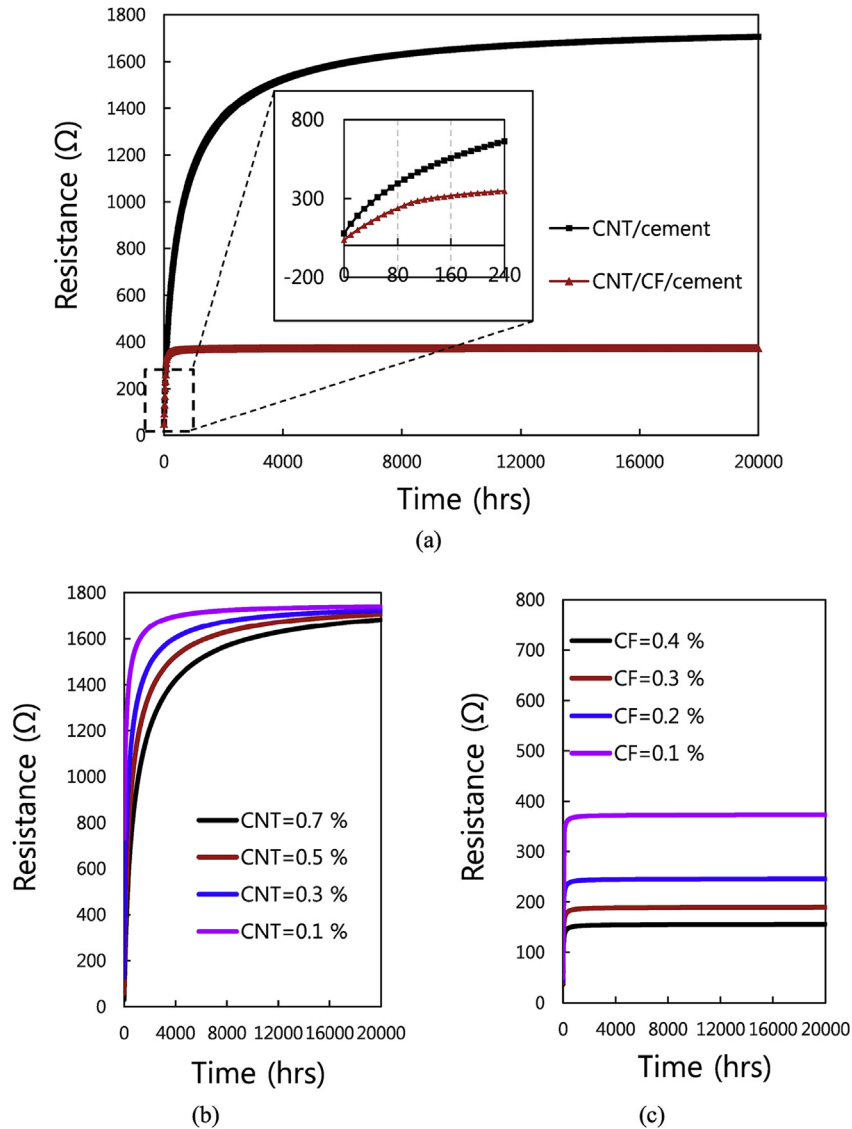


Fig. 9. The predicted electrical resistance-time curves of the composites with various conditions. (A colour version of this figure can be viewed online.)

Table 2, and the temperature over time is assumed to follow the trend line for the measurement values shown in Fig. 7(a). As depicted in Fig. 10, the present predictions match well with the experimental results for the cementitious composites, showing the potential of the model considering CNT/CF synergistic effect.

5. Concluding remarks

The heat generation and electrical characteristics of cementitious composites incorporating CNT and carbon fiber were investigated in the present study. The heat generation characteristics of the composites and the relationship between the thermal expansion and the electrical characteristics were examined under various heating conditions. The electrical resistance of composites for a longer period than the experiment was estimated based on the modified micromechanical model. The model parameters which are difficult to quantify theoretically are derived from the experimental results, and the potential of the modified model is assessed via numerical simulations and experimental comparisons. The results obtained in this study could contribute to the expansion of knowledge on the electrical and heat generation characteristics of

cementitious composites with CNT and CF, and to an increase in the applicability of the composites as floor heating and de-icing materials in construction fields.

- 1) The addition of CF improved the heat generation capability of the cementitious composites incorporating CNT, while the addition of fine aggregate decreased the capability of all specimens.
- 2) The occurrence of an inflection point was delayed by adding CF to the cementitious composites with CNT. In contrast, the electrically conductive pathways in the cementitious composites with CNT were readily damaged by thermal expansion during heating.
- 3) The heat generation and the electrical stability of the cementitious composites with CNT and CF during the long-term heating tests were improved compared to those of cementitious composites with CNT. This is possibly attributed to that an overlapped area was formed by adding the CF to the cementitious composites with CNT and reduced the damage to the electrically conductive pathways induced by the thermal expansion,

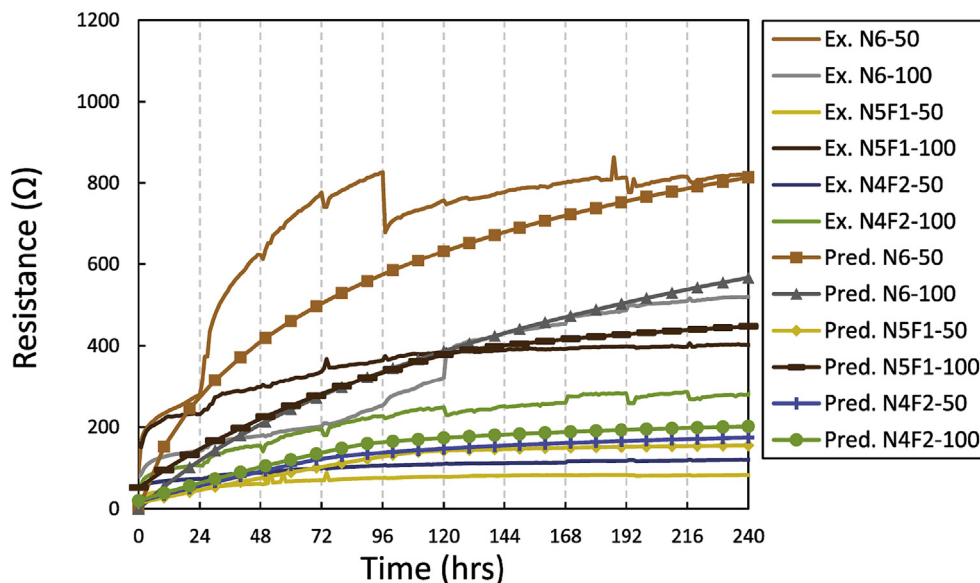


Fig. 10. The comparison between the present experimental data and predictions for overall electrical resistance vs. time responses of cementitious composites. (A colour version of this figure can be viewed online.)

Table 2

Filler volume fraction, coefficient of thermal expansion, and temperature gradient values applied to proposed model for experimental comparisons.

Specimen	CNT volume fraction, ϕ_1 (%)	CF volume fraction, ϕ_2 (%)	Coefficient of thermal expansion ($E^{-6}/^{\circ}\text{C}$)	Temperature gradient ($^{\circ}\text{C}$)
N6-50	0.786	0	18.23	$0.0108t + 43.862$
N6-100	0.593	0	9.42	$-0.0425t + 59.904$
N5F1-50	0.655	0.096	19.10	$0.0556t + 60.138$
N5F1-100	0.494	0.072	8.65	$0.0006t + 64.96$
N4F2-50	0.524	0.192	14.78	$0.0703t + 59.101$
N4F2-100	0.395	0.145	18.00	$0.0276t + 60.58$

addition hydration reactions, and internal cracking during the heating process.

- 4) The electrical resistance-time responses of the present composites with various mix proportions are predicted based on the proposed model. The present predictions match well with the experimental results for the cementitious composites, showing the predictive capability of the derived model considering CNT/CF synergy and tunneling effects.

Acknowledgements

This research was supported by the National Research Foundation of Korea (NRF) grant funded by the Korean government (Ministry of Science, ICT & Future Planning) (NRF-2015R1A2A1A10055694).

References

- [1] C.Y. Tuan, S. Yehia, Evaluation of electrically conductive concrete containing carbon products for deicing, *ACI Mater. J.* 101 (4) (2004) 287–293.
- [2] Q. Liu, E. Schlangen, Á. García, M. van de Ven, Induction heating of electrically conductive porous asphalt concrete, *Construct. Build. Mater.* 24 (7) (2010) 1207–1213.
- [3] D. Chung, Self-heating structural materials, *Smart Mater. Struct.* 13 (3) (2004) 562.
- [4] S. Wang, S. Wen, D. Chung, Resistance heating using electrically conductive cements, *Adv. Cement Res.* 16 (4) (2004) 161–166.
- [5] T. Wu, R. Huang, M. Chi, T. Weng, A study on electrical and thermal properties of conductive concrete, *Comput. Concr.* 12 (3) (2013) 337–349.
- [6] H. Li, Q. Zhang, H. Xiao, Self-deicing road system with a CNFP high-efficiency thermal source and MWCNT/cement-based high-thermal conductive composites, *Cold Reg. Sci. Technol.* 86 (2013) 22–35.
- [7] Z. Qin, Y. Wang, X. Mao, X. Xie, Development of graphite electrically conductive concrete and application in grounding engineering, *New Build. Mater.* 11 (2009) 46–48.
- [8] M. Park, J.H. Park, B. Yang, J. Cho, S.Y. Kim, I. Jung, Enhanced interfacial, electrical, and flexural properties of polyphenylene sulfide composites filled with carbon fibers modified by electrophoretic surface deposition of multi-walled carbon nanotubes, *Compos. Part A-Appl. Sci. Manuf.* 109 (2018) 124–130.
- [9] J. Wu, J. Liu, F. Yang, Three-phase composite conductive concrete for pavement deicing, *Construct. Build. Mater.* 75 (2015) 129–135.
- [10] J.-P. Salvetat, J.-M. Bonard, N. Thomson, A. Kulik, L. Forro, W. Benoit, L. Zuppiroli, Mechanical properties of carbon nanotubes, *Appl. Phys. A* 69 (3) (1999) 255–260.
- [11] S. Bal, S. Samal, Carbon nanotube reinforced polymer composites—a state of the art, *Bull. Mater. Sci.* 30 (4) (2007) 379.
- [12] F. Inam, H. Yan, M. Reece, T. Peijs, Structural and chemical stability of multiwall carbon nanotubes in sintered ceramic nanocomposite, *Adv. Appl. Ceram.* 109 (4) (2010) 240–247.
- [13] S. Musso, J.-M. Tulliani, G. Ferro, A. Tagliaferro, Influence of carbon nanotubes structure on the mechanical behavior of cement composites, *Compos. Sci. Technol.* 69 (11–12) (2009) 1985–1990.
- [14] S.Y. Kim, H.G. Jang, C.-M. Yang, B. Yang, Multiscale prediction of thermal conductivity for nanocomposites containing crumpled carbon nanofillers with interfacial characteristics, *Compos. Sci. Technol.* 155 (2018) 169–176.
- [15] G. Kim, B. Yang, K. Cho, E. Kim, H. Lee, Influences of CNT dispersion and pore characteristics on the electrical performance of cementitious composites, *Compos. Struct.* 164 (2017) 32–42.
- [16] H. Kim, I. Park, H. Lee, Improved piezoresistive sensitivity and stability of CNT/cement mortar composites with low water–binder ratio, *Compos. Struct.* 116 (2014) 713–719.
- [17] B. Han, X. Yu, E. Kwon, A self-sensing carbon nanotube/cement composite for traffic monitoring, *Nanotechnology* 20 (44) (2009), 445501.
- [18] G. Kim, F. Naeem, H. Kim, H. Lee, Heating and heat-dependent mechanical characteristics of CNT-embedded cementitious composites, *Compos. Struct.* 136 (2016) 162–170.
- [19] T. Nochaiya, A. Chaipanich, Behavior of multi-walled carbon nanotubes on the porosity and microstructure of cement-based materials, *Appl. Surf. Sci.* 257 (6) (2011) 1941–1945.

- [20] X. Chen, S. Wu, Influence of water-to-cement ratio and curing period on pore structure of cement mortar, *Construct. Build. Mater.* 38 (2013) 804–812.
- [21] F. Azhari, N. Bantia, Cement-based sensors with carbon fibers and carbon nanotubes for piezoresistive sensing, *Cement Concr. Compos.* 34 (7) (2012) 866–873.
- [22] J. Zuo, W. Yao, X. Liu, J. Qin, Sensing properties of carbon nanotube–carbon fiber/cement nanocomposites, *J. Test. Eval.* 40 (5) (2012) 838–843.
- [23] X. Xia, Y. Wang, Z. Zhong, G.J. Weng, A frequency-dependent theory of electrical conductivity and dielectric permittivity for graphene-polymer nanocomposites, *Carbon* 111 (2017) 221–230.
- [24] H. Souri, J. Yu, H. Jeon, J.W. Kim, C.-M. Yang, N.-H. You, B. Yang, A theoretical study on the piezoresistive response of carbon nanotubes embedded in polymer nanocomposites in an elastic region, *Carbon* 120 (2017) 427–437.
- [25] American Society for Testing and Materials, ASTM C778–13: Standard Specification for Standard Sand, ASTM Int, 2013.
- [26] American Society for Testing and Materials, ASTM C 109/C 109M. Test Method for Compressive Strength of Hydraulic-cement Mortars (Using 2-in. or 50-mm Cube Specimens), ASTM Int, 2013.
- [27] Agilent Technologies, Agilent U1241A and U1242A Handheld Digital Multimeters, 2012.
- [28] G. Kim, S. Park, G. Ryu, H. Lee, Electrical characteristics of hierarchical conductive pathways in cementitious composites incorporating CNT and carbon fiber, *Cement Concr. Compos.* 82 (2017) 165–175.
- [29] G. Kim, B. Yang, G. Ryu, H. Lee, The electrically conductive carbon nanotube (CNT)/cement composites for accelerated curing and thermal cracking reduction, *Compos. Struct.* 158 (2016) 20–29.
- [30] Z.D. Xiang, T. Chen, Z.M. Li, X.C. Bian, Negative temperature coefficient of resistivity in lightweight conductive carbon nanotube/polymer composites, *Macromol. Mater. Eng.* 294 (2) (2009) 91–95.
- [31] G. Wang, H. Xiao, H. Li, X. Guan, A scouring sensor by using the electrical properties of carbon nanotube-filled cement-based composite, *Sens. Smart Struct. Technol. Civ. Mech. Aerosp. Syst.* 8692 (2013) 39.
- [32] X. He, J. Du, Z. Ying, H. Cheng, X. He, Positive temperature coefficient effect in multiwalled carbon nanotube/high-density polyethylene composites, *Appl. Phys. Lett.* 86 (6) (2005), 062112.
- [33] S. Ye, Conductive concrete overlay for bridge deck deicing, *ACI Mater. J.* 97 (2) (1999) 171–182.
- [34] S. Meyers, Thermal expansion characteristics of hardened cement paste and of concrete, in: *Highway. Res. Board Proc.*, 1951.
- [35] D.-x. Xuan, Z.-h. Shui, B.-b. Cao, Investigation on thermal deformation divergence between components of cement-basted materials, *J. Wuhan Univ. Technol.* 1 (2007), 007.
- [36] R. Loser, B. Münch, P. Lura, A volumetric technique for measuring the coefficient of thermal expansion of hardening cement paste and mortar, *Cement Concr. Res.* 40 (7) (2010) 1138–1147.
- [37] B. Hao, Q. Ma, S. Yang, E. Mäder, P.-C. Ma, Comparative study on monitoring structural damage in fiber-reinforced polymers using glass fibers with carbon nanotubes and graphene coating, *Compos. Sci. Technol.* 129 (2016) 38–45.
- [38] B. Yang, J.-u. Jang, S.-H. Eem, S.Y. Kim, A probabilistic micromechanical modeling for electrical properties of nanocomposites with multi-walled carbon nanotube morphology, *Compos. Appl. Sci. Manuf.* 92 (2017) 108–117.
- [39] Y. Ngabonziza, J. Li, C. Barry, Electrical conductivity and mechanical properties of multiwalled carbon nanotube-reinforced polypropylene nanocomposites, *Acta Mech.* 220 (1–4) (2011) 289–298.
- [40] H. Jeon, J. Yu, H. Lee, G. Kim, J.W. Kim, Y.C. Jung, C.-M. Yang, B. Yang, A combined analytical formulation and genetic algorithm to analyze the nonlinear damage responses of continuous fiber toughened composites, *Comput. Mech.* 60 (3) (2017) 393–408.
- [41] B. Yang, H. Shin, H. Kim, H. Lee, Strain rate and adhesive energy dependent viscoplastic damage modeling for nanoparticulate composites: molecular dynamics and micromechanical simulations, *Appl. Phys. Lett.* 104 (10) (2014) 101901.